Journal of Applied Electrochemistry **31**: 693–702, 2001.

Electrochemical dissolution of tin in methanesulphonic acid solutions

R.A.T. DE GREEF and L.J.J. JANSSEN
Department of Electrochemical Technology, Faculty of Chemical Engineering and Chemistry, Eindhoven University of Technology, PO Box 513, 5600 MB Eindhoven, The Netherlands

Received 21 August 2000; accepted in revised form 31 January 2001

Key words: conductivity, corrosion, density, hydrogen evolution, hydrogen peroxide reduction, methane sulphonic acid, oxygen reduction, tin, viscosity

Abstract

High-rate electroplating of tin on a moving steel strip is generally carried out in cells with dimensionally stable anodes. To obtain a matt tin deposit a concentrated acidic tin methanesulphonate solution containing a small concentration of sulphuric acid is used. The concentrated tin methanesulphonate solution is prepared by dissolution of tin particles with oxygen in a special column. To describe this dissolution process electrode reactions (namely, reduction of oxygen, hydrogen peroxide and hydrogen ions on a tin electrode and oxidation of tin) were studied using electrochemical techniques. It was concluded that on tin, oxygen is almost entirely reduced to water and that H_2O_2 cannot corrode tin directly, but its decomposition products, for instance oxygen, can. The exchange current density and the charge transfer coefficient for the investigated electrode reactions are estimated. The dissolution of tin by oxygen is determined by the kinetic parameters of the oxygen reduction reaction and by the mass transfer of (i) dissolved oxygen to and (ii) Sn^{2+} ions from the tin electrode surface. Hydrogen evolution can be neglected during the dissolution of tin in the presence of oxygen. Moreover, it was found that the rate of tin corrosion increases with (i) increasing H^+ concentration, (ii) oxygen concentration, (iii) convection intensity and (iv) temperature. It is likely that the tin surface is not covered with oxygen during corrosion in pure methanesulphonic acid solutions, but an oxide layer may be present on the tin surface during oxygen corrosion in pure sulphuric acid solutions. This oxide layer may hinder the oxygen corrosion of tin.

List of symbols

A_e	electrode surface area (m^2)
b	Tafel slope based on E/log i curve (V)
$b°$	modified Tafel slope (V) based on E/ln i curve; $b° = 0.435\ b$
c	concentration (mol m^{-3})
$c^0_{O_2}$	oxygen solubility in a solution at an oxygen pressure of 1 bar
D	diffusion coefficient ($m^2\ s^{-1}$)
d_e	diameter of disc electrode (m)
E	electrode potential (V)
E_r	reversible electrode potential (V)
$E°$	standard electrode potential (V)
E_{act}	activation energy (J mol^{-1})
E_{cor}	corrosion potential (V)
F	faradaic constant (96 487 C mol^{-1})
f	rotation rate of electrode (s^{-1})
h	slope of log i–T^{-1} curve (K)
I	current (A)
i	current density (A m^{-2})
i_0	exchange current density (A m^{-2})
i°_0	standard exchange current density (A m^{-2})
i_g	limiting current density (A m^{-2})
i_{gd}	limiting diffusion current density (A m^{-2})
i_{cor}	corrosion current density (A m^{-2})
K_a	ionization constant of an acid (mol dm^{-3})
k_t	mass transfer coefficient (s^{-1})
n	number of electrons involved in electrode reaction (mol^{-1})
R	gas constant (8.3144 J $mol^{-1}K^{-1}$)
R_{cor}	corrosion resistance ($\Omega\ m^2$)
R_Ω	ohmic resistance between working electrode and tip of Luggin capillary
T	temperature (K)
t	time (s)

Greek symbols

α	charge transfer coefficient of reaction (–)
α_{cor}	corrosion charge transfer coefficient (–)
δ_N	thickness of Nernst layer (m)
η	overpotential (V)
η	dynamic viscosity (kg $m^{-1}\ s^{-1}$)
η_Ω	Ohmic overpotential (Ω)
κ	conductivity ($\Omega^{-1}\ m^{-1}$)
λ	equivalent conductivity ($\Omega^{-1}\ m^{-1}\ mol^{-1}$ kg)
ν	kinematic viscosity ($m^2 s^{-1}$)
ρ	density (kg m^{-3})
ω	angle rotation rate (s^{-1})

Subscripts/superscripts

a	anodic reaction
b	bulk of solution
c	cathodic reaction
e	electrode surface
H_2	hydrogen formation or $H_2 \leftrightarrow 2H^+$ redox couple
H_2O_2	hydrogen peroxide reduction
HSA	sulfuric acid
HMSA	methanesulfonic acid
n	potential scan in the negative potential
O_2	oxygen reduction or $O_2 + 4H^+ \leftrightarrow 2H_2O$ redox couple
ox	oxidizing agent
p	potential scan in the positive direction
r	reversible
red	reducing agent
ref	reference condition
Sn	tin
T	temperature
w	water
η	fixed overpotential

1. Introduction

Matt tin deposits are generally formed from acidic Sn(II) baths. Modern electroplating lines use alkyl sulphonic acids. Methanesulphonic acid (HMSA) is gaining favour and is an attractive alternative to tetrafluoboric acid [1]. Most insoluble anodes are based on titanium coated with noble metals, in particular IrO_2/Ta_2O_5/Ti anodes operate satisfactorily in alkyl solutions containing Sn(II) alkylsulphonate and sulphonic acids [1]. Sn(II) loss is replenished externally. In practice the tin(II) solution is pumped from the plating bath to a dissolution reactor filled with tin particles and fed with oxygen gas, and thereafter the more concentrated tin(II) solution is pumped back to the plating bath.

From the Pourbaix diagram for the tin–water system [2] it can be deduced that in an acidic solution containing dissolved oxygen the dissolution of tin can take place by two different corrosion processes, *viz*. the hydrogen corrosion and the oxygen corrosion. No results about both corrosion types for tin in HMSA have been previously reported. In contrast, extensive information on the corrosion and its subprocesses (oxidation of Sn to Sn(II), hydrogen evolution and the reduction of oxygen) in inorganic acids, like sulphuric acid, is available [3].

Since the earlier studies gave conflicting results, Quintin and Hagymas [4] have reinvestigated hydrogen evolution on tin in H_2SO_4 solutions. They found that the cathodic charge transfer coefficient is $\alpha_{H_2} = 0.5$ and the exchange current density is about $i_0 = 10^{-5}$ A m^{-2}. The corrosion of tin in acid solutions is quite fast if oxygen is present in the corroding medium [5]. Delahay [6] studied the reduction of oxygen on a Sn-plate electrode in a phosphate buffer of pH 6.9. He found that oxygen is practically completely reduced to water at potentials more negative than -0.30 V vs SHE.

The kinetics of the electron transfer in the Sn^{2+}/Sn system were studied extensively [5, 7]. Based on the critical evaluation of the results [5], it was concluded that for Sn oxidation in HCl and H_2SO_4 solutions at 293 K the apparent anodic charge transfer coefficient α_a and the standard exchange current density i_0^0 are about 2 and 0.8 A cm^{-2}, respectively. The activation polarization for Sn deposition on polycrystalline and single crystal tin is so low that the concentration polarization is usually predominant in steady-state polarization measurements [7].

The aim of this research is to determine the electrochemical parameters of the various electrode reactions for corrosion of tin in HMSA solutions with and without the presence of oxygen.

2. Experimental details

The experiments were performed in a thermostatic electrochemical cell using a rotating disc electrode as working electrode, a 5 cm^2 platinum counter electrode placed at a distance of about 10 cm from the working electrode, and a saturated calomel reference electrode. The latter was connected to the cell via a Luggin capillary, which was filled with a salt bridge (Agar Agar/H_2SO_4 or HMSA). The working electrode was a tin disc with a geometric surface area of 28.4 mm^2 and surrounded by a Perspex cylinder with a wall thickness of 1.0 mm. The tin disc electrode was polished mechanically with 0.3 μm alumina. After polishing alumina was removed by rinsing and placing the electrode in an ultrasonic water bath. After a series of experiments and, in some cases, after each experiment in a series, the tin electrode was repolished to improve the reproducibility of experimental results.

The hydrogen evolution was also investigated on a stationary upwards facing Sn electrode with a geometric surface area of 11.3 cm^2. This electrode was located at the bottom of one branch of a thermostatic H-shaped electrolysis cell. In this case the potential was scanned between -0.6 and -1.0 or -1.2 V and the stand-by potential was -0.6 V to prevent Sn corrosion.

The working electrode compartment of the cell was air-tight. After adding the 'air-free' solution into the cell, a flow of nitrogen gas saturated with water vapour was passed through the solution for about 30 min until just before the measurement started. During the measurement under 'oxygen-free' conditions the electrolyte was kept under a blanket of water-saturated N_2. To saturate

the solution oxygen gas saturated with water vapour was passed through the solution for 30 min before the start of the measurement and was passed over the solution during the measurement.

Current–potential curves were recorded with a digital potentiostat (Autolab, PGSTAT 20, EcoChemie). The applied scan rate of potential was 10 mV s^{-1}. The potential scan in the positive potential direction will be referred to the 'positive scan' and that in the negative direction as 'negative scan'. The temperature was 308 K unless otherwise mentioned. Special care was paid to the ohmic potential drop correction. The ohmic resistance R_Ω of the solution between the Luggin capillary tip and the working electrode was determined by two methods: impedance spectroscopy and the calculation method described in [8, 9], in which it is assumed that the charge transfer coefficient is constant. It was found that for HMSA solutions both methods gave practically the same result. Only for H_2SO_4 solutions was a clear difference obtained. Usually the inaccuracy in R_Ω determined with the first method was relatively large (~10%). Therefore, the second method was preferred, since in this case a constant charge transfer coefficient is expected.

3. Results

3.1. *Physical properties and solubility of oxygen in aqueous HMSA solutions*

Very few literature data are available for the density, viscosity and conductivity of HMSA solutions.

3.1.1. *Density*

The density of HMSA solutions at 298 and 308 K was determined by the usual method. Solutions with various HMSA concentrations were made from a stock HMSA solution containing 13.017 molality HMSA (Ronastan TP, Shipley Ronal). The results at 308 K are given in Table 1. From the experimental results it was found that at both 298 and 308 K: $\rho - \rho_w = 40.5\, c_{HMSA} - 2.5\, c_{HMSA}^2$ for solutions with a molality $c_{HMSA} \leqslant 1.64$ m.

3.1.2. *Viscosity*

The dynamic viscosity η of a HMSA solution was determined with a Ubbelohde viscosimeter 530 10/J (Schott viscosimeter, type CT 1450, AVS 350). The kinematic viscosity $v = \eta/\rho$ was calculated using the density ρ from Table 1. Results for HMSA solutions with different concentrations are shown in Table 1. From these results it follows that at $T = 308$ K $v = 0.727 \times 10^{-6} + 0.107 \times 10^{-6}\, c_{HMSA}$ $m^2\ s^{-1}$. Moreover, it was found that the slope of the log v/T^{-1} curve for $c_{HMSA} = 0.2481$ m was practically equal to the slope of the log v_w/T^{-1} curve.

3.1.3. *Conductivity*

The conductivity of HMSA solutions was determined with a conductivity radiometer (type CDM 230), where a conductance cell with a cell constant of 1.17 m^{-1} was used. Part of the results are given in Table 1. From the experimental results it followed that the equivalent conductivity for HMSA solutions at 308 K $\lambda = 47.4 - 14.14\, c_{HMSA}^{1/2}$ $\Omega^{-1}\ m^{-1}\ mol^{-1}$ kg, where c_{HMSA} is given in mol per kg water and the temperature dependence of the equivalent conductance is given by $\lambda_T = \lambda_{298} \exp\left[-1075\left(\frac{1}{T} - \frac{1}{298}\right)\right]$ for a 0.2481 as well as a 1.614 m HMSA solution.

3.1.4. *Solubility of oxygen*

The solubility of oxygen was determined for HMSA solutions of various concentrations at 308 K after saturation by air. The oxygen content was measured with an oxygen indicator (model 26072, sensor 21152, Orbisphere Laboratories). The saturation solubility of oxygen in water at 308 K and saturated with pure oxygen at a pressure of 1 bar is 1.026 mM [10]. From the experimental results [11] and taking into account the oxygen content in air (i.e., 21%) the solubility of oxygen, C_{O_2}, in various HMSA solutions at 308 K and 1 bar an oxygen gas pressure was evaluated and is given in Table 1.

3.2. *Hydrogen evolution*

To determine the electrochemical parameters for the hydrogen evolution, it was preferred to carry out voltammetric experiments in 'oxygen-free' solutions. Using the procedure described in Section 2, it was impossible to decrease the oxygen concentration in the solution to a level where its influence on the potential–current relation at low current densities was negligible. Fortunately, this influence can be eliminated to a large extent. Steady state of the tin electrode surface was

Table 1. Density, conductivity, kinematic viscosity and oxygen solubility at $P_{O_2} = 1$ bar in HMSA solutions of different concentrations at 308 K

c_{HMSA}/mol kg^{-1}	ρ/kg m^{-3}	$v \times 10^6$/$m^2\ s^{-1}$	$\kappa/\Omega^{-1}\ m^{-1}$	$c^0_{O_2}$/mol m^{-3}
0	994	0.727	–	1.026
0.1008	1001	0.741	4.24	1.052
0.2481	1007	0.757	10.05	0.986
0.5161	1017	0.787	19.02	0.957
1.0630	1037	0.842	33.93	0.952
1.6410	1059	0.905	46.40	0.952

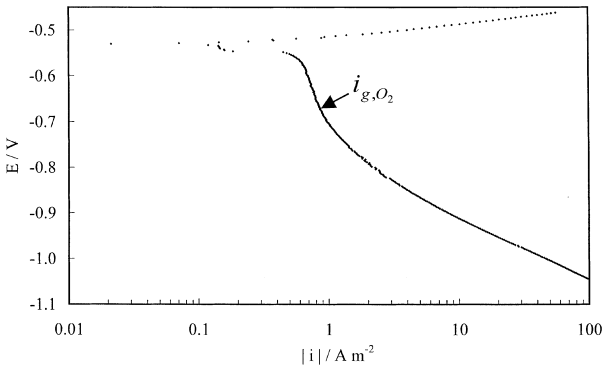

Fig. 1. Potential as a function of log|*i*| at a tin electrode in an 'oxygen-free' 0.248 m HMSA solution at 308 K and 16 rps for a cathodic potential scan.

practically obtained after one full potential scan. Generally, the voltammograms for the second and the third scan were practically the same and the latter was used to determine the electrochemical parameters. A typical $E/\log|i|$ plot for a positive potential scan is shown in Figure 1 for a rotating tin disc electrode in an 'oxygen-free' HMSA solution.

It was found that the direction of the potential scan has practically no effect on the relationship between potential and anodic current and a slight effect on that between potential and cathodic current, where the cathodic current for the cathodic potential scan is smaller than that for the positive potential scan. The $E/\log|i|$ curve shows a bending point at $E = -0.67$ V, where $i = 0.83$ A m^{-2}. The curve in the cathodic current region can be explained by the occurrence of two reactions, namely, the reduction of oxygen and the evolution of hydrogen. It is likely that the current at the bending point is practically equal to the diffusion limited current density for oxygen reduction. This means that $i_{H_2} = |i| - |i_{g,O_2}|$ at $E < E_{cor}$. In Figure 2 the potential E is plotted versus $\log i_{H_2}$. This Figure shows a straight line over a large potential range.

Similar results were obtained with stationary tin disc electrodes in unstirred 'oxygen-free' solutions. In this case, the stand-by potential was -0.6 V vs SCE to prevent tin corrosion and the potential was scanned between -0.6 and -1.0 or -1.2 V. It was found that the i_{g,O_2} was clearly smaller than that for the rotating disc electrode.

The exchange current density i_{0,H_2} for hydrogen evolution is usually determined by extrapolating the $E/\log i_{H_2}$-curve to E_{r,H_2} calculated from the Nernst equation and using the ionization constant of HMSA, that is, $K_{HMSA} = 10^{1.9}$ mol dm^{-3} [12].

The selection of the parameters was determined by possible conditions of the industrial tin oxidation process with oxygen. The composition of the solution, in particular the HMSA and H_2SO_4 concentration, is very important.

Pure HMSA solutions with concentrations 0.1 to 1.64 m, a 0.124 m H_2SO_4 solution and HMSA–H_2SO_4 solutions with $c_{HMSA} = 0.248$ m and $c_{HAS} = 0$ to 0.1 m were used. Experiments were carried out with a rotating, as well as a stationary, electrode. For pure HMSA solutions Figure 3 shows the Tafel slopes $b_{H_2,p}$ and $b_{H_2,n}$ for the scan range -0.6 to -1.0 V as a function of HMSA concentration. $b_{H_2,p}$ is about 10% larger than $b_{H_2,n}$ and $b_{H_2,p}$ as well as $b_{H_2,n}$ are practically constant at $c_{HMSA} > 0.2$ m and increase with decreasing c_{HMSA} at $c_{HMSA} < 0.2$ m. Moreover, it was found that $b_{H_2,p}$ and $b_{H_2,n}$ are much closer to each other for the scan range -0.6 to -1.2 V. It is reasonable to conclude that for pure HMSA solutions with $c_{HMSA} > 0.2$ m, the Tafel slope b_{H_2} under stationary conditions is 117 mV, corresponding to a charge transfer coefficient $\alpha_{c,H_2} = 0.48$.

For a 0.248 m HMSA solution containing different H_2SO_4 contents it was found that the H_2SO_4 content has practically no effect on the Tafel slope. The Tafel slopes $b_{H_2,p}$ and $b_{H_2,n}$ for a 0.124 m H_2SO_4 solution are 125 and 112 mV, respectively.

In Figure 4 the current densities $i_{H_2,p}$ and $i_{H_2,n}$ at a fixed overpotential (650 mV) are plotted against the HMSA concentration for pure HMSA solutions on a semi-logarithmic scale. This overpotential was chosen to minimize the effect of corrections upon the potential–current curve due to oxygen reduction and ohmic potential drop.

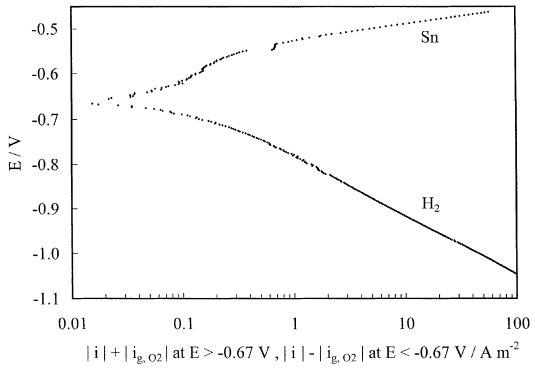

Fig. 2. Potential as a function of $\log(|i| + |i_{g,O_2}|)$ at $E > E_{cor}$ and as a function of $\log(|i| - |i_{g,O_2}|)$ at $E < E_{cor}$, where $E_{cor} = E$ at $i = 0$ A m^{-2} at a tin electrode in an 'oxygen-free' 0.248 m HMSA solution at 308 K and 16 rps and for the cathodic potential scan.

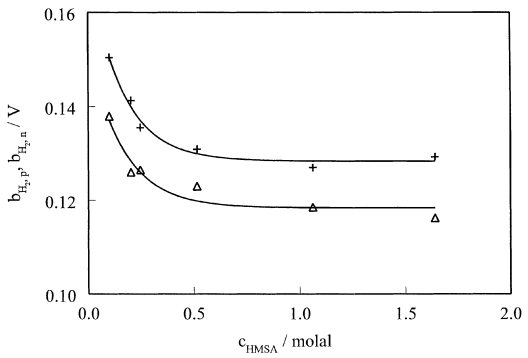

Fig. 3. Tafel slope $b_{H_2,p}$ (+) and $b_{H_2,n}$ (△) for hydrogen evolution on a tin electrode in pure HMSA solutions with various HMSA concentrations and at 308 K.

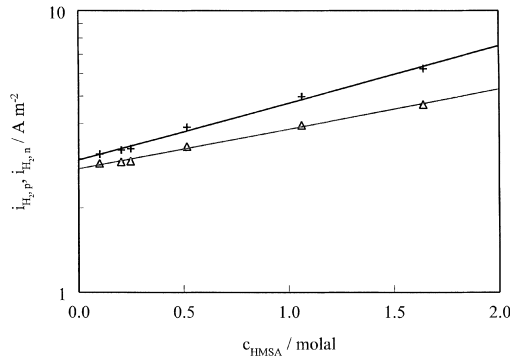

Fig. 4. Current densities $i_{H_2,p}$ (+) and $i_{H_2,n}$ (△) at an overpotential of 650 mV for hydrogen evolution on a tin electrode in pure HMSA solutions with various HMSA concentrations and at 308 K.

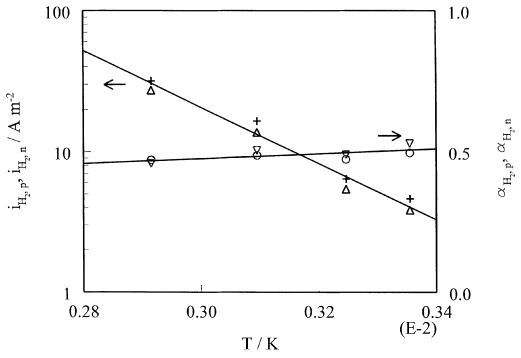

Fig. 6. Current density i_{H_2} at $\eta = 650$ mV and the transfer coefficient α_{H_2} for both scan directions as a function of the reverse of the absolute temperature on a semi-logarithmic scale for a tin electrode in a 1.64 m HMSA solution.

Figure 4 shows that log i_{H2} for both scan directions increases linearly with c_{HMSA}. To obtain reliable results, the exchange current density $i_{0,H}$ for the hydrogen evolution on tin was calculated from i_H at $\eta = 650$ mV, using $\log i_{0,H_2} = \log i_{H_2} - (\eta/b_{H_2})$ for both scan directions and $\log i_{0,H_2} = (\log i_{0,H_2,p} + \log i_{0,H_2,n})/2$. The calculated i_{0,H_2} is represented in Figure 5. In addition i_{0,H_2} was also calculated using the stationary Tafel slope b_{H_2} at $c_{HMSA} > 0.2$ m, that is, 117 mV for all HMSA concentrations. The result is also given in Figure 5. The two relations between i_{0,H_2} and c_{HMSA} are quite different, particularly at low c_{HMSA} and the reaction order in H^+-ions is very low.

Experiments were also carried out for a 0.248 and a 1.64 m HMSA solution at various temperatures. Figure 6 shows results for a 1.64 m HMSA solution. From this Figure and from the results for a 0.248 m HMSA solution it follows that the charge transfer coefficient α_{c,H_2} being $(\alpha_{c,H_2,p} + \alpha_{c,H_2,n})/2$ does not depend on temperature and is equal to 0.48. Moreover, the slopes $h_{H_2,p}$ and $h_{H_2,n}$ of the log $i_{H_2,p}/T^{-1}$ and the log $i_{H_2,n}/T^{-1}$ curve at an overpotential of 650 mV are equal. Using the slope $h_{H_2} = -0.434\ E_{act,\eta}/R$ the activation energy $E_{act,\eta}$ for hydrogen evolution at $\eta = 650$ mV was determined. Since $E_{act,\eta} = E_{act,r} - \alpha_{c,H_2} F\eta$, the activation energy $E_{act,r}$ for hydrogen evolution at the reversible potential was found to be 110 kJ mol^{-1}. Practically the same results were obtained for a 0.248 m HMSA solution [13].

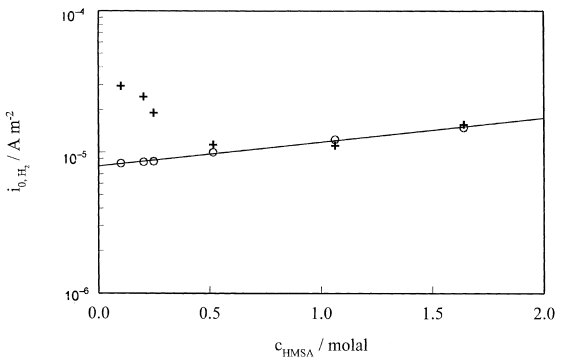

Fig. 5. Exchange current density i_{0,H_2} calculated with the Tafel slope found for each i/E curve (+) as well as a constant Tafel slope of 117 mV (○), for hydrogen evolution on a tin electrode in pure HMSA solutions with various HMSA concentrations and at 308 K.

3.3. *Tin dissolution*

The voltammograms obtained for 'oxygen-free' solutions are the most suitable to determine the electrochemical parameters for electrochemical tin dissolution. Since the solutions were not completely free from oxygen, it might be necessary to take the oxygen reduction current into account. To minimize the effect of the oxygen reduction current on the Tafel slope for tin oxidation, only the anodic current density range above 4 i_{g,O_2} was used to determine the Tafel slope. Both extreme limits for anodic Sn dissolution were examined, that is, $i_{Sn} = |i|$ and $i_{Sn} = |i| + |i_{g,O_2}|$. The $E/\log|i|$ curve was smooth with a constant slope at $|i| > 4\,|i_{g,O_2}|$ and a decreasing slope at $|i| < |i_{g,O_2}|$ with decreasing potential (Figure 2). The $E/\log(|i| + |i_{g,O_2}|)$ curve was an S-shaped curve indicating a significant contribution of oxygen reduction during Sn dissolution. From this it was concluded that the effect of oxygen reduction on the $E/\log|i|$ curve at $|i| > 4|i_{g,O_2}|$ is negligible.

It was found that the Tafel slope for tin dissolution does not depend on the HMSA concentration for 0.1 to 1.6 m for HMSA solutions and on the H_2SO_4 concentration for 0.248 m HMSA solutions containing up to 0.1 m H_2SO_4. Moreover, the direction of the potential sweep has a very slight effect on the Tafel slope. From all experimental data it followed that the Tafel slope for tin dissolution in HMSA solutions is about 31.7 mV; this is only slightly higher than 30.6 mV being 2.3 $RT/2F$ at $T = 308$ K for the Sn/Sn^{2+} redox couple with reversible behavior. The Tafel slope b_{Sn} for the 0.122 m H_2SO_4 solution is clearly larger than that for the HMSA solutions, if only the potential correction for the ohmic drop in the solution is taken into account. In this case the experimental $E/\log i$ curve for Sn dissolution was a strongly bent curve in the scan range -0.7 to -0.3 V (not corrected for ohmic potential drop). The impedance measurements showed an Argand plot with two

semicircles. It is likely that the diameter of the semicircle in the high frequency range is equal to the ohmic resistance of the oxide layer on the Sn electrode. Applying this resistance for additional correction to the measured potential, the resulting $E/\log i_{Sn}$ curve was a straight line over the relevant potential range -0.50 to -0.44 V. When the α = constant calculation method [8, 9] was applied, then practically the same Tafel slope (31 mV) was found, where the potential was corrected for the sum of both resistances, that is, the solution between the electrode and the tip of the Luggin capillary and that one for the oxide layer in the electrode.

From experiments with a 0.248 m HMSA solution at various temperatures it was found that the Tafel slope for Sn dissolution is proportional to the absolute temperature T. This agrees with the fact that this Tafel slope is determined by the Nernst equation.

3.4. *Oxygen reduction*

3.4.1. *Limiting current density*

Voltammograms for a rotating disc electrode in an 'oxygen-free' and an oxygen saturated HMSA solution are represented in Figure 7 which shows a clear current plateau for the oxygen reduction. A series of experiments was carried out, first with increasing and thereafter with decreasing rotation rate. It was found that the limiting current density for oxygen reduction i_{g,O_2} is proportional to the square root of the rotation rate.

Figure 8 shows i_{g,O_2} as a function of HMSA concentration for a rotating Sn electrode with a stationary surface. It is observed that i_{g,O_2} decreases with increasing c_{HMSA}. Some voltammograms were measured with the same rotating Sn electrode in a 0.124 m H_2SO_4 and a 0.248 m HMSA solution and both solutions were saturated with oxygen. It was found that i_{g,O_2} was practically the same for both solutions.

3.4.2. *Electrochemical parameters*

Figure 7 shows that E_{cor} is determined by the reduction of oxygen and the oxidation of tin. Assuming the two reactions do not interfere, it is possible to obtain the current density for oxygen reduction, i_{O_2} at potentials higher than -0.60 V, that is, $i_{O_2} = |i_2| + |i_1|$, where $i_2 = i$ for the oxygen saturated solution and $i_1 = i$ for the 'oxygen-free' solution. To eliminate the effect of concentration polarization on the Tafel slope for oxygen reduction $i_{O_2} i_{g,O_2}/(i_{g,O_2} - i_{O_2})$ was plotted against E on a semi-logarithmic scale. This procedure gave no reliable and acceptable Tafel slope. This means that both processes affect each other.

To calculate the corrosion current density, i_{cor}, a Tafel slope of 120 mV at 298 K is assumed for the oxygen reduction. This is the Tafel slope for oxygen reduction on noble metals, Au, Ag, Hg and carbon in clearly acidic solutions (pH < 2) [14]. As a first approximation $\alpha_{c,O_2} n = 0.5$ for the oxygen reduction on tin in HMSA solutions will be acceptable.

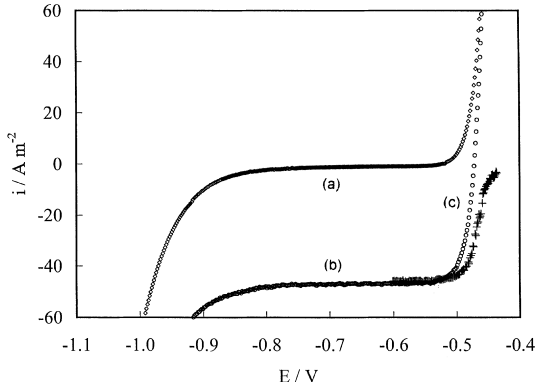

Fig. 7. Potential–current density curves for a rotating tin disc electrode in an 'oxygen-free' (a) and an oxygen saturated (b) 0.248 m HMSA solution at 308 K and a rotation rate of 16 rps and for the positive scan. Curve (c) is obtained from both curves.

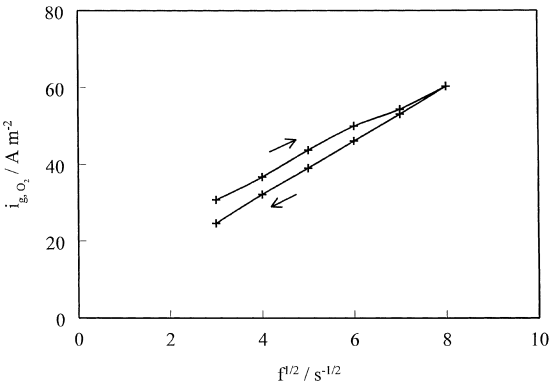

Fig. 8. The limiting current density for oxygen reduction on a rotating tin electrode at 308 K and a rotation rate of 16 rps against the HMSA concentration of pure HMSA solutions saturated with oxygen. The nature of the electrode surface is in a stationary state.

3.5. *Corrosion resistance and potential*

From the experimental i/E curves E_{cor}, i_{g,O_2} and the slope of the i/E curve at E_{cor} were determined. The direction of the potential scan had practically no effect on the experimental results. Therefore, average values are presented in this and the following Sections. In Figure 9 the corrosion resistance R_{cor} and E_{cor} for a rotating Sn electrode in pure HMSA solutions saturated with oxygen is given as a function of the HMSA concentration. R_{cor} and E_{cor} decrease with increasing HMSA concentration. The effects of mass transport on the corrosion potential and corrosion resistance were studied. R_{cor} and E_{cor} decreased with increasing rotation rate. For oxygen saturated HMSA–H_2SO_4 solutions with 0.248 m HMSA and H_2SO_4 concentrations up to 0.1 m it was found that R_{cor} is practically independent of the H_2SO_4 concentration and E_{cor} decreases significantly with increasing H_2SO_4 concentration, that is, from -0.474 to -0.500 V for $c_{H_2SO_4}$ from 0 to 0.1 m. Corrosion resistance and potential were also determined for a Sn electrode in a 0.124 m H_2SO_4 solution saturated

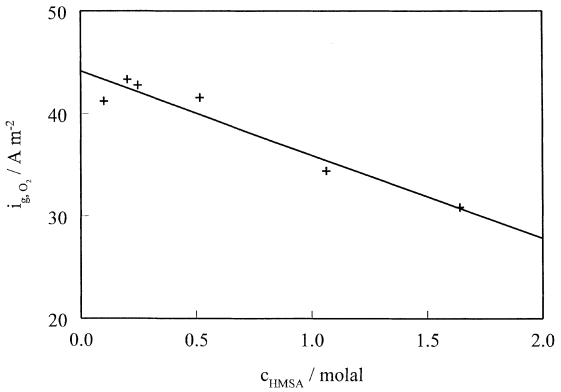

Fig. 9. The corrosion resistance (+) and the corrosion potential (△) against HMSA concentration for a tin disc electrode in pure HMSA solutions saturated with oxygen and at 308 K and 16 rps.

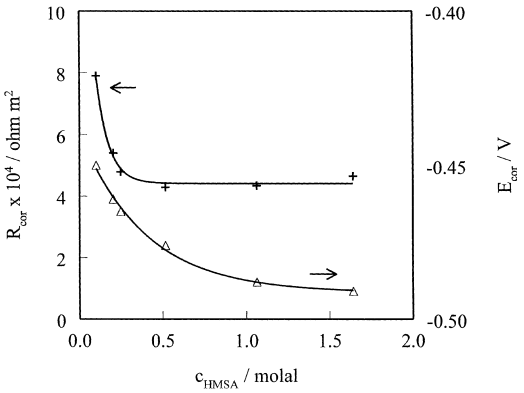

Fig. 10. Corrosion current density (+) and ratio $i_{cor}/i_{g,O_2}$ (△) against the concentration of HMSA for a Sn electrode in pure HMSA solutions saturated with oxygen and at 308 K and 16 rps.

with oxygen and at a rotation rate of 16 rps. It was also found that $R_{cor} = 50 \times 10^{-6}$ Ω m^2, $i_{g,O_2} = 45.42$ A m^{-2} and $E_{cor} = -0.438$ V.

Experiments were also carried out at various temperatures for a 0.248 m and a 1.64 m HMSA solution saturated with oxygen. It was found that for both solutions the product R_{cor} and i_{g,O_2} is practically independent of temperature.

3.6. *Corrosion current density*

To obtain the corrosion current density from R_{cor}, it is necessary to know the rate-determining step for the corrosion process and, in some cases, the kinetic and/or the mass transfer parameters for the participating reactions.

From the results for hydrogen evolution, Sn oxidation and oxygen reduction, it follows that the tin corrosion in oxygen containing acidic solution is mostly determined by oxidation of tin and reduction of oxygen and that hydrogen corrosion of tin can be neglected.

In Appendix I the relation between i_{cor} and R_{cor} is given for tin corrosion, under the hypothesis that tin oxidation is a fast reaction and oxygen reduction is determined by kinetic and mass transfer parameters.

In Section 3.4.2 it is assumed that $\alpha_{c,O_2} = 0.5$ hence $b_{c,O_2} = 0.122$ V at 308 K. The corrosion current density i_{cor} at 308 K was calculated using $b_{a,Sn} = 0.031$ V and $b_{c,O_2} = 0.122$ V, the experimental R_{cor} and i_{g,O_2}.

Corrosion current density as a function of HMSA concentration and rotation rate are shown in Figures 10 and 11. It follows that i_{cor} increases with increasing HMSA concentration and rotation rate. Moreover, the ratio $i_{cor}/i_{g,O_2}$ is also represented in both Figures. $i_{cor}/i_{g,O_2}$ increases with increasing HMSA concentration and decreases with increasing rotation rate.

For a tin RDE in an oxygen saturated 0.124 m H_2SO_4 solution at 16 rps and 308 K it was found that $i_{cor} = 4.29$ A m^{-2} and the ratio $i_{cor}/i_{g,O_2} = 0.094$. Both values are significantly smaller than those for the pure HMSA solution with the same molality.

To show the effect of b_{O_2} on the calculated i_{cor}, calculations were carried out with $b_{O_2} = 0.060$ V. It was found that i_{cor} for $b_{O_2} = 0.060$ V is about 20% higher than that for $b_{O_2} = 0.122$ V.

3.7. *Tin corrosion by hydrogen peroxide*

Since hydrogen peroxide can be formed by reduction of oxygen, some experiments were carried out with 0.248 m HMSA solutions containing various H_2O_2 contents. Figure 12 shows R_{cor} and E_{cor} as a function of H_2O_2 concentration. For the 'oxygen-free' and H_2O_2 free solution it was found that $R_{cor} = 0.12$ Ω m^2 and $i_{cor} = 0.18$ A m^{-2}. From these results and Figure 12 it follows that R_{cor} decreases strongly with increasing $c_{H_2O_2}$ in the range 0 to 2.5 mol m^{-3} and only slightly at $c_{H_2O_2} >$ 2.5 mol m^{-3}. The corrosion potential increases strongly with increasing $c_{H_2O_2}$.

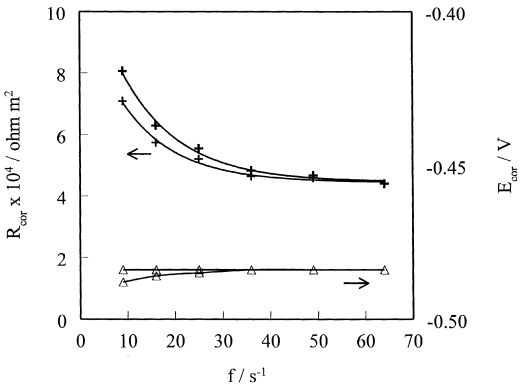

Fig. 11. Corrosion current density (+) and ratio $i_{cor}/i_{g,O_2}$ (△) against the rotation rate for a Sn electrode in 0.248 m HMSA saturated with oxygen and at 308 K. Arrow on curve indicates the direction of change of rotation rate during the series of experiments.

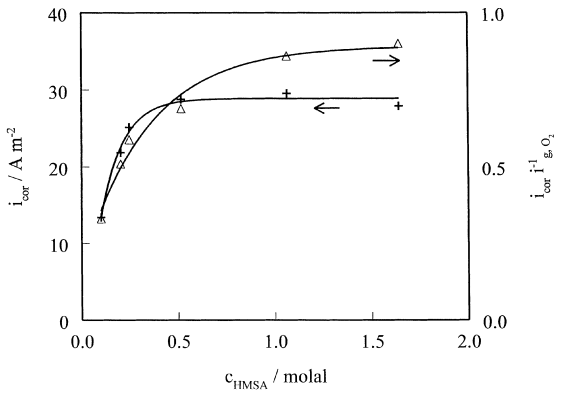

Fig. 12. Corrosion resistance R_{cor} (+) and corrosion potential (△) as a function of H_2O_2 concentration for a Sn electrode in 'oxygen-free' 0.248 m HMSA and at 308 K and 16 rps.

4. Discussion

4.1. *Hydrogen evolution*

The results show that the Tafel slope b_{H_2} (Figure 3) and the current density i_{H_2} at a fixed overpotential (Figure 4) depend on the direction of the potential scan during the measurement. This indicates that the nature of the tin electrode surface depends significantly on the potential, in particular on the maximum and minimum potential during the potential scan experiments.

The mean Tafel slope b_{H_2} is close to 120 mV for HMSA solutions with $c_{HMSA} > 0.2$ m and corresponds to a charge transfer for coefficient $\alpha_{H_2} = 0.5$. This agrees with the results given for a Sn electrode in sulphuric acid solutions [4, 15] and for similar electrode materials like Hg and Zn [5].

Figure 5 shows that i_{0,H_2} increases with increasing HMSA concentration. For a 0.5 m HMSA solution $i_{0,H_2} = 1.0 \times 10^{-5}$ A m^{-2}. This value is of the same order of magnitude as found for 0.5 m H_2SO_4, that is, 2.2×10^{-5} A m^{-2} [15]. It can be concluded that the anion MSA^- shows practically no interaction with the tin electrode just as the HSO_4^- or SO_4^{2-} anion. So, the specific effect of the methanesulphonic anion upon i_{0,H_2} is limited and its value is mainly determined by the solution pH.

It is unlikely that for an electrode surface with a constant nature i_{0,H_2} increases with decreasing H^+ concentration as shown in Figure 5 using the experimental Tafel slopes at $c_{HMSA} < 0.5$ m. Probably, oxides formed on the Sn electrode at $c_{HMSA} < 0.5$ m will effect b_{H_2} as well as i_{0,H_2}.

4.2. *Tin oxidation*

The experimental Tafel slope b_{Sn} is 31.7 mV, being only slightly larger than 30.6 mV corresponding to 2.3 $RT/2F$ at 308 K. If this small difference is correct, then the kinetic parameters of anodic tin dissolution have a small effect on b_{Sn}. In Appendix II the i/E relation is deduced for Sn oxidation in a solution containing practically no Sn^{2+} ions. From this relation it follows that several parameters must be known to obtain the standard exchange current density for the Sn–Sn^{2+} redox couple, $i^\circ_{0,Sn}$.

Assuming a two-electron electrode reaction ($n = 2$), $\alpha_a = \alpha_c = 0.5$, $k_t = 6.32 \times 10^{-5}$ m s^{-1} (determined for a rotating electrode at 16 rps), $c_{Sn,ref} = 1000$ mol m^{-3}, and $E^\circ_{Sn} = -0.136$ V vs NHE the current density, i_{Sn}, was calculated as a function of electrode potential and $E - E^\circ_{Sn}$ was plotted versus log i_{Sn} for various $i^\circ_{0,Sn}$. Comparing the experimental Tafel slope with the calculated, it was found that $i^\circ_{0,Sn}$ will be about 5×10^3 A m^{-2}, in reasonable agreement with $i^\circ_{0,Sn}$ for sulphate solutions [5].

4.3. *Reduction of oxygen*

4.3.1. *H_2O_2 and/or H_2O formation*

The potential–current density curve for oxygen reduction on tin shows a clear plateau over a wide potential range (Figure 7). Oxygen can be reduced to either water and/or hydrogen peroxide. This ratio can be determined by comparing the experimental i_{g,O_2} with the diffusion limiting current density calculated by the Levich equation, that is, $i_{gd,O_2} = 0.62\, nFD_{O_2}^{2/3} \nu^{-1/6} c_{O_2,b} \omega^{1/2}$. Since i_{g,O_2} is proportional to $\omega^{1/2}$ (Section 3.4.1) it follows that i_{g,O_2} is determined by diffusion.

For a 0.284 cm^2 Sn RDE rotated at 16 rps the parameter n was calculated for various HMSA solutions using $c_{O_2,b}$ from Table 1, the Stokes–Einstein equation, $D_{O_2,W} = 2.90 \times 10^{-9}$ m^2 s^{-1} [16] and the experimental i_{c,g,O_2}. It was found that the mean $n = 3.4$. Two limiting values for n are possible: 2 for the reduction of oxygen to hydrogen peroxide and 4 for that to water.

Similar experiments were carried out with a rotating platinum electrode in 'oxygen-free' and oxygen saturated HMSA solutions and at 308 K and a rotation rate of 16 rps. Although the voltammograms for Pt in oxygen saturated HMSA solutions showed clearly shaped shoulders, it was possible to determine a limiting current density for oxygen reduction. From the results presented in [13] and using the Levich equation, it was found that $n = 1.6$ for the oxygen reduction on Pt. Since the minimum value for $n = 2$, it is likely that the difference between $n = 1.6$ and $n = 2$ may be caused by the nonideal behaviour of the rotating disc electrode and/or deviations in the other parameters used in the Levich equation. Since i_{g,O_2} for Sn is also about a factor of 2 higher than i_{g,O_2} for Pt, it is concluded that on Sn oxygen is almost completely reduced to water. This was also obtained for Sn in 0.2 M. KCl at pH 6.9 [17].

4.3.2. *Kinetic parameters for oxygen reduction on tin*

The relation between i_{O_2} and E at high overpotential is given by

$$\left|\frac{i_{O_2} i_{g,O_2}}{i_{g,O_2} - i_{O_2}}\right| = i_{0,O_2} \exp\left(-\alpha_{c,O_2} n \frac{F}{RT}(E - E_{r,O_2})\right) \quad (1)$$

Since at the corrosion potential $i_{O_2} = i_{cor}$, from the corrosion current density and the ratio $i_{cor}/i_{g,O_2}$ (Figure 12) the factor on the left side of Equation 1 was calculated at E_{cor}. The reversible potential E_r for the H_2O–O_2 redox couple is obtained from the Nernst equation. It has been shown that it is reasonable to accept $\alpha_c n = 0.5$ (Section 3.4.1). Introducing these parameters into Equation 1 it was found that i_{0,O_2} increases slightly with increasing HMSA concentration, that is, $i_{0,O_2} = 1.80 \times 10^{-10}\, c_H^{0.22}$ A m^{-2}. The order of magnitude of i_{0,O_2} on tin agrees with that for noble metals, where also $\alpha_c n$ is about 0.5 [14].

The Tafel slope b_{O_2} and extrapolated i_{0,O_2} depend strongly on the presence of an oxide layer on the electrode surface; for example, for Pt $i_{0,O_2} = 8.5 \times 10^{-9}$ A m^{-2} and $b_{O_2} = 0.120$ V and for a Pt–O alloy $i_{0,O_2} = 3.2 \times 10^{-5}$ A m^{-2} and $b_{O_2} = 0.300$ V [14]. This large difference is caused by the overpotential drop over the oxide layer. From impedance spectra and potential–current curves it was concluded that an oxide layer is present on Sn in 0.124 m H_2SO_4 and in the potential range -0.5 to 0 V. In this potential range an oxide layer was not detectable for Sn in HMSA solutions.

4.4. *Tin corrosion*

In oxygen saturated HMSA solutions tin corrosion due to H_2 evolution is negligible and the rate of mass transfer for oxygen to the tin electrode strongly affects the rate of tin corrosion. The ratio $i_{cor}/i_{g,O_2}$ decreases with increasing rotation rate (Figure 11) and increases with increasing HMSA concentration (Figure 12). From these results and since the exchange current density for the Sn–Sn^{2+} redox couple is very high, it is concluded that in oxygen containing HMSA solutions i_{cor} is determined by both the kinetic parameters for the oxygen reduction and the oxygen mass transfer. For an oxygen saturated H_2SO_4 solution i_{cor}, as well as the ratio $i_{cor}/i_{g,O_2}$, are significantly smaller than for HMSA solutions. This means that in H_2SO_4 solutions the kinetic parameters for oxygen reduction dominate the tin corrosion. It is also possible that an oxide layer present on tin at the corrosion potential will play a significant role, not only on the oxygen reduction, but also on the anodic Sn dissolution.

In HMSA–H_2SO_4 mixtures with a ratio $c_{HMSA}/c_{H_2SO_4}$ higher than 2.5 and $c_{HMSA} = 0.25$ m the effect of H_2SO_4 concentration on tin corrosion is practically absent. Probably, under these conditions no oxide layer is present on Sn at E_{cor}.

The corrosion resistance due to H_2O_2 increases strongly with increasing $c_{H_2O_2}$ in the range 0 to 2.5 mol m^{-3} and only slightly at $c_{H_2O_2} > 2.5$ mol m^{-3} (Section 3.7). A corrosion current density, that is, 62 A m^{-2} due to H_2O_2 corrosion was obtained at $c_{H_2O_2} = 30$ mol m^{-3}. This value is a factor of 3.7 higher than i_{cor} obtained with an oxygen saturated 0.248 m HMSA solution, where $c_{O_2} = 0.99$ mol m^{-3}.

It was found that $i_{g,H_2O_2}^{-1}$ increases practically linearly with increasing $c_{H_2O_2}^{-1}$. Assuming $D_{O_2} = D_{H_2O_2}$ and H_2O_2 is reduced to H_2O it was calculated that the limiting diffusion current density for H_2O_2 reduction, i_{gd,H_2O_2}, on a rotating electrode at 16 rps in 0.248 m HMSA solutions containing 30 mol m^{-3} H_2O_2 is equal to 634 A m^{-2}, being a factor of about 2 higher than the experimental i_{g,H_2O_2}. The corrosion potential in 0.248 m HMSA solutions with $c_{H_2O_2} = 30$ mol m^{-3} is practically equal to that in 0.24 m $HMSO_4$ saturated with oxygen and the limiting current density for H_2O_2 reduction is also obtained at practically the same potential as that for oxygen reduction. If the difference in concentrations is taken into account, it may be concluded that tin corrosion in the presence of H_2O_2 is determined by decomposition of H_2O_2 to oxygen on the tin surface and a direct reduction of H_2O_2 on Sn is not likely.

5. Conclusions

(i) The rate of tin corrosion in HMSA solutions containing oxygen is determined by the oxygen corrosion and the hydrogen corrosion is negligible.

(ii) For the hydrogen evolution on tin it was found that the standard exchange current density increases slightly with increasing HMSA concentration, being about 10^{-5} A m^{-2}, the charge transfer coefficient is 0.48 and the activation energy at the reversible hydrogen potential is 110 kJ mol^{-1}.

(iii) For the oxidation of Sn to Sn(II) it was found that the standard exchange current density is about 5×10^3 A m^{-2}. So, the mass transfer of Sn(II) practically determines the potential–current density relation.

(iv) For the oxygen reduction it was assumed that the first step is rate-determining and a one-electron reaction and that the charge transfer coefficient is 0.5. The exchange current density for the oxygen reduction is then given by $1.80 \times 10^{-10}\, c_H^{0.22}$ A m^{-2}, where c_H is the H^+ concentration in mol kg^{-1}.

(v) The oxygen corrosion of tin is determined by the mass transfer of oxygen to the Sn electrode, as well as the kinetic parameters of oxygen reduction on the Sn electrode.

References

1. M. Jordan, 'The Electrodeposition of Tin and its Alloys' (Eugen G. Leuze, Saulgan/Württ, 1995).
2. M. Pourbaix, 'Atlas of Electrochemical Equilibria in Aqueous Solutions' (Pergamon, Oxford, 1966).
3. Gmelins, 'Handbuch der Anorganischen Chemie', System-Nummer 46, Teil B, (Verlag Chemie GmbH, Weinheim, 1971).
4. A.J. Bard, 'Encyclopedia of Electrochemistry of the Elements', Vol. IX, part A (Marcel Dekker, New York Basel, 1973), p. 448.
5. A.J. Bard, 'Encyclopedia of Electrochemistry of the Elements', Vol. 4 (Marcel Dekker, New York, 1975), p. 223.

6. P. Delahay, *J. Electrochem. Soc.* **97** (1950) 205.
7. S. Meibuhr, E. Yeager, A. Kozawa and F. Hovorka, *J. Electrochem. Soc.* **110** (1963) 190.
8. N. Munichandraiah and S. Sathyanarayana, *J. Appl. Electrochem.* **17** (1987) 33.
9. L.J.J. Janssen and P.D.L. van der Heijden, *J. Appl. Electrochem.* **25** (1995) 126.
10. Landolt–Börnstein, 'Physikalisch-Chemische Tabellen', 2. Teil, Bandteil b, Lösungsgleichgewichte I (Springer Verlag, 1962), p. 20.
11. K. Schetz, private communication.
12. W.J. Tuszynski, *Elektrokhimiya* **26** (1990) 249.
13. R.A.T. de Greef, Graduation report, TUE (1999).
14. A.J. Bard, 'Encyclopedia of Electrochemistry of the Elements', Vol. 2 (Marcel Dekker, New York, 1974), p. 208.
15. K. Gossner, *Z. Phys. Chem. N.F.* **36** (1963) 392.
16. R.T. Ferrel and D.M. Himmelblau, *J. Chem. Eng. Data* **12** (1967) 111.
17. P. Delahay, *J. Electrochem. Soc.* **97** (1950) 205.

Appendix I. Derivation of equation for i_{cor}

The relation between the corrosion resistance R_{cor} and the corrosion current density is deduced for a special case. It is assumed that tin oxidation is a fast reaction, so that the i_{Sn}/E curve is determined by concentration polarisation. From the Nernst equation and the first Fick's law it is deduced that in the absence of Sn^{2+} ions in the bulk solution:

$$i_{Sn} = \frac{2FD_{Sn}}{\delta_N}\exp\left(\frac{2F}{RT}(E - E^\circ_{Sn})\right) \tag{1}$$

and

$$\left(\frac{di}{dE}\right)_{Sn} = \frac{i_{Sn}}{b^\circ_{Sn}} \tag{2}$$

where $b^\circ_{Sn} = RT/2F$. The Tafel slope $b_{Sn} = 2.3\, b^\circ_{Sn}$.

Moreover, it is assumed that the reduction of oxygen on tin at E_{cor} is determined by kinetic as well as diffusion transport parameters. The diffusion limiting current density is also obtained from the experimental i/E curve. Since the oxygen reduction is usually a very slow reaction, it is likely that the partial anodic current for the oxygen–water redox couple at E_{cor} can be neglected. It can be shown that then

$$\left|\frac{i_{O_2} i_{g,O_2}}{i_{g,O_2} - i_{O_2}}\right| = i_{0,O_2}\exp\left(-\alpha_{c,O_2} n\frac{F}{RT}(E - E_{r,O_2})\right) \tag{3}$$

and

$$\left(\frac{di_{O_2}}{dE}\right)_{E_{cor}} = b^\circ_{O_2}\frac{i_{O_2}(i_{g,O_2} - i_{O_2})}{b^\circ_{O_2} i_{g,O_2}} \tag{4}$$

where $b^\circ_{O_2} = RT/(\alpha_{c,O_2} nF)$. The Tafel slope $b_{O_2} = 2.3\, b^\circ_{O_2}$.

Since

$$i_{cor} = |i_{Sn,E_{cor}}| = |i_{O_2,E_{cor}}| \tag{5}$$

it can be shown that at E_{cor}:

$$\left|\left(\frac{di}{dE}\right)_{E_{cor}}\right| = \left|\left(\frac{di_{Sn}}{dE}\right)_{E_{cor}}\right| + \left|\left(\frac{di_{O_2}}{dE}\right)_{E_{cor}}\right| \tag{6}$$

and

$$\left(\frac{di}{dE}\right)_{E_{cor}} = \frac{i_{cor}}{b^\circ_{Sn}} + \frac{i_{cor}(i_{g,O_2} - i_{cor})}{b^\circ_{O_2} i_{g,O_2}} = R^{-1}_{cor} \tag{7}$$

Rearrangement of Equation 7 gives:

$$\frac{i^2_{cor}}{b^\circ_{O_2} i_{g,O_2}} - \left(\frac{1}{b^\circ_{Sn}} + \frac{1}{b^\circ_{O_2}}\right) i_{cor} + R_{cor} = 0 \tag{8}$$

From Equation 8 it is deduced:

$$i_{cor} = \frac{(b^\circ_{Sn} + b^\circ_{O_2}) i_{g,O_2}}{2b^\circ_{Sn}} - \frac{i_{g,O_2} b^\circ_{c,O_2}}{2}\sqrt{\left(\frac{1}{b^\circ_{Sn}} + \frac{1}{b^\circ_{O_2}}\right)^2 - \frac{4}{b^\circ_{O_2} i_{g,O_2} R_{cor}}} \tag{9}$$

If b°_{Sn}, $b^\circ_{O_2}$, i_{gd,O_2} and R_{cor} are well known, then i_{cor} can be calculated.

Appendix II. Derivation of i/E relation for the Sn oxidation in a solution containing practically no Sn^{2+} ions

For the reaction $Sn \rightarrow Sn^{2+} + 2e^-$ the current density is given by:

$$i_{Sn} = i_{0,Sn}\left(\exp\left(\alpha_a n\eta\frac{F}{RT}\right) - \frac{c_{Sn,e}}{c_{Sn,ref}}\exp\left(-\alpha_c n\eta\frac{F}{RT}\right)\right) \tag{1}$$

where $c_{Sn,e}$ is the concentration of Sn^{2+} ions at Sn electrode, $c_{Sn,ref}$ the concentration of Sn^{2+} ions in the reference Sn^{2+} solution, being 1 M or 1000 mol m^{-3}, $\eta = E - E_r$ and $E_r = E^\circ$ since $c_{Sn,ref} = 1$ M.

According to Fick's law and since $n = 2$:

$$i_{Sn} = 2FD\frac{(c_{Sn,b} - c_{Sn,e})}{\delta_N} \tag{2}$$

Since $c_{Sn,b} \approx 0$ from Equation 2 and $D/\delta_n = k_t$ it follows that

$$c_{Sn,e} = \frac{i_{Sn}}{2k_t} \tag{3}$$

Introducing Equation 3 for c_e in Equation 1 and after rearrangement, gives

$$i^{-1}_{Sn} = \left[i^\circ_{0,Sn}\exp\frac{\alpha_a nF(E - E^\circ)}{RT}\right]^{-1} + \left[2Fk_t c_{Sn,ref}\exp\frac{(\alpha_c + \alpha_a)nF(E - E^\circ)}{RT}\right]^{-1} \tag{4}$$